European Polymer Journal 126 (2020) 109566

Contents lists available at ScienceDirect

European Polymer Journal

journal homepage: www.elsevier.com/locate/europolj

Synthesis of high molecular weight poly(*n*-butyl acrylate) macromolecules *via se*ATRP: From polymer stars to molecular bottlebrushes

Izabela Zaborniak[a,b], Paweł Chmielarz[a,b,*], Michael R. Martinez[b], Karol Wolski[c], Zongyu Wang[b], Krzysztof Matyjaszewski[b,*]

[a] Department of Physical Chemistry, Faculty of Chemistry, Rzeszow University of Technology, Al. Powstańców Warszawy 6, 35-959 Rzeszow, Poland
[b] Department of Chemistry, Carnegie Mellon University, 4400 Fifth Ave., Pittsburgh, PA 15213, United States
[c] Faculty of Chemistry, Jagiellonian University, Gronostajowa 2, 30-387 Krakow, Poland

ARTICLE INFO

Keywords:
Star-shaped polymers
Bottlebrushes
Electrochemically-mediated atom transfer radical polymerization
Atomic force microscopy imaging

ABSTRACT

Poly(*n*-butyl acrylate) (PBA) branched polymers have interesting properties and potential applications as super soft materials and pressure sensitive adhesives. Herein, star and comb polymers with long PBA sidechains were synthesized by a simplified electrochemically-mediated ATRP (*se*ATRP) utilizing ca. 100 ppm of Cu catalyst. Grafting-from (or core-first) synthesis of PBA stars using a multifunctional sucrose initiator (Sucrose-Br_8) was best controlled using moderately negative applied potentials. This method was also applied to the synthesis of molecular bottlebrushes with long sidechains to a relatively high conversion. The prepared molecular bottlebrushes had low dispersity, with length distributions of 1.01 for the shorter bottlebrushes (backbone DP = 316) and 1.03 for the longer brushes (backbone DP = 1,632), as determined by atomic force microscopy (AFM) imaging.

1. Introduction

Compared to linear polymers of the same molecular weight, graft/comb polymers have less chain entanglement, lower viscosity, and a higher local concentration of polymer chain ends [1,2]. These properties enable graft polymers to be used as drug delivery vehicles, lubricants, molecular nanotemplates, supersoft materials, and stimuli-responsive materials [3–8]. Comb/graft polymer architectures can be synthesized by the "grafting-through" (polymerization of macromonomers) [9,10], "grafting-onto" (coupling sidechains onto a backbone) [11,12], or "grafting-from" (polymerization from a multifunctional macroinitiator) methods [12,13]. The grafting-onto and grafting-through methods can leave behind residual linear impurities which can be difficult to separate from a chemically similar graft polymer. The "grafting-from" method alleviates this issue by polymerizing "small" monomers from an already prepared multifunctional macroinitiator.

Controlled radical polymerization (CRP) techniques, such as reversible addition-fragmentation chain transfer polymerization (RAFT) [14,15], nitroxide mediated polymerization (NMP) [16–18], and atom transfer radical polymerization (ATRP) [19,20], have significantly simplified the synthesis of complex grafted architectures by the grafting-from method. A well-controlled CRP will suppress most radical termination (RT) by reducing radicals' concentration *via* equilibration with dormant polymer species. Excessive bimolecular radical termination by coupling will lead to the formation of higher molecular weight products, and eventually crosslinking, if a grafting-from polymerization is uncontrolled. The synthesis of large, multifunctional, molecular bottlebrushes by the grafting-from method has been previously conducted under dilute conditions with low activity catalysts used at high concentrations to suppress the undesired termination. Grafting-from polymerizations have seen some success by polymerization in dispersed media or by promoting alternative termination pathways [13,21].

Attempts have been made to reduce copper loading in grafting-from ATRP to prepare polymer stars and bottlebrushes with chemical reducing agents (ARGET ATRP) [22,23], external radical sources (ICAR ATRP) [24], zero-valent metals (SARA ATRP) [24,25], electrical current (*e*ATRP) [26–30], and UV light (photoATRP) [31]. Lowering the concentration of Br-Cu^{II}/L catalyst in grafting-from ATRP while maintaining control over polymerization presents a unique challenge in the synthesis of well-defined graft polymers. A lower concentration of Br-Cu^{II}/L can lead to slower deactivation and less efficient initiation at the beginning of a grafting-from polymerization [32,33]. Inefficient deactivation can broaden distribution of side chains, causing long side

* Corresponding authors at: Department of Physical Chemistry, Faculty of Chemistry, Rzeszow University of Technology, Al. Powstańców Warszawy 6, 35-959 Rzeszow, Poland (P. Chmielarz). Department of Chemistry, Carnegie Mellon University, 4400 Fifth Ave., Pittsburgh, PA 15213, United States (K. Matyjaszewski).
E-mail addresses: p_chmiel@prz.edu.pl (P. Chmielarz), km3b@andrew.cmu.edu (K. Matyjaszewski).

https://doi.org/10.1016/j.eurpolymj.2020.109566
Received 28 January 2020; Received in revised form 10 February 2020; Accepted 11 February 2020
Available online 12 February 2020

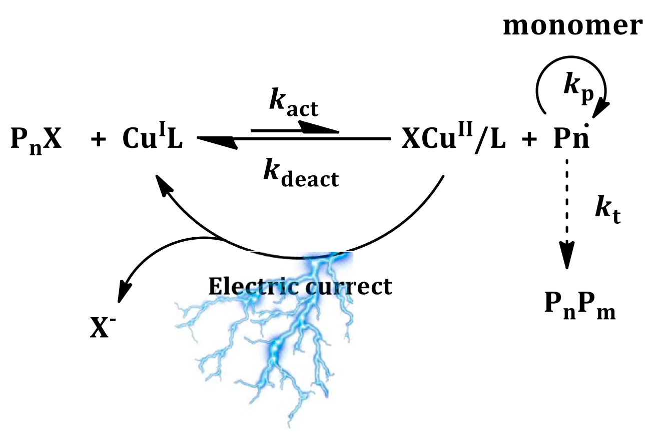

Scheme 1. Mechanism of *e*ATRP (P_nX - initiator, Cu^IL - activator, XCu^{II}/L - deactivator, $P_n^{\cdot}$ - growing radicals, P_nP_m - terminated polymer chain, X^- - halogen anion, k_{act} - activation rate constant, k_{deact} - deactivation rate constant, k_p - propagation rate constant, k_t - termination rate constant).

chains to sterically shield nearby initiators and reduce graft density [34]. A lower graft density will alter the bulk and solution conformations of a graft polymer and will affect the materials properties [35,36].

It is important to investigate new methods of grafting-from synthesis which could both decrease bimolecular RT and produce well-defined graft polymers at low loadings of $Br\text{-}Cu^{II}/L$. Polyacrylate stars of low molecular weight prepared by grafting-from SARA ATRP could reach near quantitative conversion by ^1H NMR without coupling detectable by gel permeation chromatography (GPC) [25]. Similarly, simplified electrochemically mediated solution ATRP (*se*ATRP) with low ppm of $Br\text{-}Cu^{II}/L$ was employed to form poly(*n*-butyl acrylate) (PBA) polymer stars up to moderately high conversion (~80%) with little evidence of coupling by gel permeation chromatography (GPC) [28]. Both methods relied on a judicious selection of polymerization conditions to compensate for lower loadings of copper catalyst (see Scheme 1).

Electrochemically mediated ATRP (*e*ATRP) allows for highly precise tuning of the Cu^I/Cu^{II} ratio by variation of the applied potential (E_{app}) and current (I) [37,38]. A more negative E_{app} gives a higher Cu^I/Cu^{II} ratio, which results in a higher rate of propagation (R_p) and can also lead to an increased rate of catalyzed radical termination if formation of organometallic species is favored [39]. Decreasing $Br\text{-}Cu^{II}/L$ will also raise dispersity and lower initiation efficiency [40].

In this work, the effect of the applied potential in the simplified electrochemically mediated ATRP of *n*-butyl acrylate was investigated. The findings were then utilized to synthesize high molecular weight polymer stars and bottlebrushes with long arms from multifunctional sucrose (Sucrose-Br_8) core and poly(2-(2-bromoisobutyryloxy)ethyl methacrylate) (PB*i*BEM) backbone.

2. Results and discussion

2.1. Synthesis of PBA stars

The sucrose-based octafunctional ATRP initiator (Scheme S1, Figs. S1 and S2, $M_{n,app}$ = 1,534.3, $Đ$ = 1.07) was prepared and utilized to synthesize polymer stars as shown in Scheme S3. A series of polymerizations were conducted to examine the effect of the applied potential (E_{app}, $E_{app} = E_{pc}$-30 mV, $E_{app} = E_{pc}$-80 mV, $E_{app} = E_{pc}$-140 mV and $E_{app} = E_{pc}$-170 mV, where E_{pc} is cathodic peak potential, Fig. S7) on grafting-from polymerization kinetics (Table 1, Figs. 1 and S9). Each *se*ATRP polymerization exhibited a rapid decay of the cathodic current at the beginning of the polymerization due to the initial presence of only $Br\text{-}Cu^{II}/L$ deactivator. Then, the equilibrium $[Cu^{II}]/[Cu^I]$ ratio was (Table S2) adjusted by the applied E_{app} to achieve constant current (Fig. S8).

Table 1
Effect of applied potential on *se*ATRP polymerization of BA from Sucrose-Br_8 octafunctional initiator.[a]

Entry	E_{app} [b] [V]	$[Cu^I]/[Cu^{II}]$	conv[c] [%]	k_p^{app} [c] [h^{-1}]	$M_{n,th}$ [d] ($\cdot 10^{-3}$)	$DP_{n,th}$ [c] (arm)	$M_{n,app}$ [e] ($\cdot 10^{-3}$)	M_w/M_n [e]	$M_{n,app}$ [g] ($\cdot 10^{-3}$)	$DP_{n,app}$ [f] (arm)	M_w/M_n [g]	LMW impurities (wt%)
S1	E_{pc}-30 mV	77	60	0.048 **0.159**[h]	586.0	570	373.1	1.09	63.9	499	1.05	9.3
S2	E_{pc}-80 mV	92	66	0.057 **0.214**[h]	644.4	627	330.6	1.11	85.7	669	1.04	8.4
S3	E_{pc}-140 mV	88	65	0.055 **0.196**[h]	634.7	617	374.0	1.09	66.2	517	1.07	8.4
S4	E_{pc}-170 mV	80	61	0.050 **0.189**[h]	592.8	580	221.6	1.17	68.7	536	1.07	9.0

[a] General reaction conditions: $[BA]_0/[Sucrose\text{-}Br_8]_0/[Cu^{II}Br_2/TPMA]_0$ = 950/1/0.1, T = 50 °C; V_{tot} = 25 mL; t = 20 h; $[BA]_0$ = 3.6 M; $[CuL]_0$ = 105 ppm; Constant potential *se*ATRP (WE = Pt, CE = Al, RE = SCE).
[b] E_{app} were selected based on CV analysis of $Cu^{II}Br_2$/TPMA catalytic complexes (Fig. S7).
[c] Monomer conversion, apparent rate constant of propagation (k_p^{app}) and apparent theoretical degree of polymerization of monomer unit per arm ($DP_{n,theo}$) were determined by NMR [10].
[d] $M_{n,th} = ([BA]_0/[Sucrose\text{-}Br_8]_0) \times conversion \times M_{BA} + M_{Sucrose\text{-}Br8}$.
[e] Apparent M_n and M_w/M_n were determined by GPC.
[f] $DP_{n,app}$ (per arm) = $M_{n,app}/M_{BA}$ [27].
[g] Apparent M_n and M_w/M_n of the arms cleaved from the star polymers executed by GPC [27].
[h] Apparent rate constant of propagation at the initial stage of the polymerization reaction.

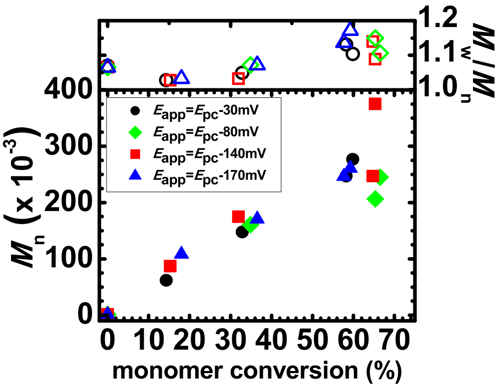

Fig. 1. M_n and M_w/M_n *vs.* monomer conversion showing the effect of applied potential on the synthesis of macromolecular star-like polymers with sucrose core *via se*ATRP.

In an *e*ATRP, more negative potential causes larger cathodic currents and thus provides faster R_p and thereby larger k_p^{app} [27]. In the absence of mass transfer limitations, R_p is directly proportional to the E_{app} and Cu^I/L to Br-Cu^{II}/L ratio [41]. When a highly negative potential is applied, the diffusion of catalyst to the working electrode surface becomes rate limiting. This can be observed as the point when R_p becomes independent on η ([$\eta = E_{app} - E_{1/2}$; $E_{1/2} = (E_{pc} + E_{pa})/2$]) and reaches a plateau; the application of more negative E_{app} values does not increase the polymerization rate [41]. This phenomenon was observed during preparative electrolysis when BA was grafted from the multifunctional Sucrose-Br_8 initiator under potentiostatic conditions.

Increasing the Cu^I/Cu^{II} ratio resulted in a small increase of polymerization rate with comparable control. When the applied potential was increased from E_{pc}-30 mV to E_{pc}-80 mV (Entries S1 and S2), the Cu^I/Cu^{II} ratio was increased from 10 to 11. This resulted in an increase in k_p^{app} from 0.159 to 0.214 h^{-1} and a small decrease of arm dispersity from M_w/M_n = 1.05 to 1.04. An even more negative E_{app} of E_{pc}-140 mV (Entry S3) kept the Cu^I/Cu^{II} ratio at 11, resulting in a slightly lower k_p^{app} of 0.196 h^{-1}. This can be attributed to the applied current reaching the upper limit of mass transport at the working electrode. High molecular weight shouldering and higher M_w/M_n values were observed for polymerizations conducted at E_{pc}-140 mV and E_{pc}-170 mV, indicating radical termination was more prominent after the overpotential was achieved (Figs. S10c and S10d) [27]. The predicted percent of chains terminated by biradical termination was estimated using the dead chain fraction (DCF) and is listed in the supplementary information (Table S3). All polymerizations from the Sucrose-Br_8 core were calculated to have less than 1% of chains terminated by radical termination.

Low molecular weight (LMW) impurities were observed in the polymerization product (Fig. S11). Their content increased with time – suggesting transfer to solvent, monomer or more attributed to preparative electrolysis – to an electrolyte were significant (Fig. S11e). The low molecular weight impurity prevented accurate assessment of number of arms by cleavage experiments, resulting in the overestimation of the initiation efficiency values. Branched architectures prepared by grafting-from ATRP under ppm concentrations of copper could have lower initiation efficiency than analogous reactions at higher catalyst loadings. Employing a low concentration of Br-Cu^{II}/L can cause non-uniform deactivation in a grafting-from polymerization, which can lower initiation efficiency due to uneven growth of sidechains [33].

Summarizing these results, an E_{app} at ~ E_{pc}-80 mV had the highest k_p^{app} and lowest M_w/M_n out of all tested conditions in the *se*ATRP of *n*-butyl acrylate from octafunctional Sucrose-Br_8 cores. These conditions were then utilized to prepare molecular bottlebrushes with relatively long sidechains using the same approach.

2.2. Synthesis of molecular bottlebrushes

The synthesis of bottlebrushes by grafting-from *se*ATRP was carried with two multifunctional linear ATRP macroinitiators, PB*i*BEM$_{316}$ (Scheme S2, Table S1, entry 1, Figs. S3 and S4, M_n = 88,200, $Đ$ = 1.12) and PB*i*BEM$_{1632}$ (Scheme S2, Table S1, entry 2, Figs. S5 and S6, M_n = 455,000, $Đ$ = 1.28), using E_{pc}-80 mV in the presence of 105 ppm of Cu/TPMA catalyst. The reactions are outlined in Table 2.

Synthesis of both P(B*i*BEM-*g*-(PBA))$_{316}$ and P(B*i*BEM-*g*-(PBA))$_{1632}$ bottlebrushes exhibited excellent control (Entries B1 and B2). Both reactions had linear first-order kinetic plots (Figs. 2a and 3a, respectively) and $M_{n,app}$ increased with conversion. GPC traces appear to be monomodal, indicating insignificant termination by coupling (Figs. 2c and 3c, respectively). $M_{n,app}$ of prepared bottlebrushes was significantly lower than $M_{n,th}$ due to the large difference in hydrodynamic volume of P(B*i*BEM-*g*-(PBA)) bottlebrushes and linear polystyrene used for GPC calibrations. The molecular brushes had low dispersity of 1.07 for P(B*i*BEM-*g*-(PBA))$_{316}$ and 1.18 for P(B*i*BEM-*g*-(PBA))$_{1632}$, respectively. The results confirm *se*ATRP could be utilized to prepare well-defined molecular bottlebrushes with minimal bimolecular radical termination.

However, again low molecular weight impurities were observed in the polymerization products (Figs. 13d and 14d). This prevented accurate assessment of initiation efficiency in grafting-from synthesis. Reaction **B1** showed 22 wt% of LMW impurities. The P(B*i*BEM-*g*-(PBA))$_{1632}$ bottlebrush with shorter arms had only 2 wt% of homopolymer impurities (**B2**, Fig. S14d). Nevertheless, sidechain cleavage

Table 2
Preparation of high molecular weight bottlebrushes with the use of macromolecular initiators.[a]

Entry	$[BA]_0/[BiBEM]_0/[Cu^{II}Br_2/TPMA]_0$	DP_{target}	Conv[b] [%]	k_p^{app} [b] [h^{-1}]	$M_{n,th}$ [c] ($\cdot 10^{-3}$)	$DP_{n,th}$ [b] (arm)	$M_{n,app}$ [d] ($\cdot 10^{-3}$)	M_w/M_n [d]	$M_{n,app}$ [f] ($\cdot 10^{-3}$)	$DP_{n,app}$ [e] (arm)	M_w/M_n [f]	LMW impurities (wt%)
B1	500/1/0.05[g]	500	33	0.127	6,707.4	163	645.0	1.11	20.8	163	1.32	22
B2	60/1/0.05[h]	60	34	0.127	4,685.9	20	945.0	1.30	4.31	34	1.07	2

[a] General reaction conditions: T = 50 °C; V_{tot} = 25 mL; t = 3.25 h, except entry 2: t = 3.5 h; $[BA]_0$ = 0.73 M; entry 1: $[MI]_0$ = 4.6 μM calculated per 316 Br initiation sites, entry 2: $[MI]_0$ = 7.5 μM calculated per 1632 Br initiation sites; [$Cu^{II}Br_2$/TPMA] = 0.08 mM; 105 ppm. Constant potential *se*ATRP (WE = Pt, CE = Al, RE = SCE); E_{app} = −0.286 V (E_{app} = E_{pc}-80 mV), except entry 2: E_{app} = -288 mV (E_{app} = E_{pc}-80 mV), E_{app} were selected based on CV analysis of $Cu^{II}Br_2$/TPMA catalytic complexes (Figs. S13a and S14a).
[b] Monomer conversion, apparent rate constant of propagation (k_p^{app}) and apparent theoretical degree of polymerization of monomer unit per arm ($DP_{n,theo}$) were determined by NMR [41].
[c] $M_{n,th}$ = ($[BA]_0/[MI]_0$) × conversion × M_{BA} + M_{MI}.
[d] Apparent M_n and M_w/M_n were determined by GPC.
[e] $DP_{n,app}$ (per arm) = $M_{n,app}/M_{BA}$ [27].
[f] Apparent M_n and M_w/M_n of the chains cleaved from the molecular bottlebrushes determined by GPC.
[g] MI: PB*i*BEM$_{316}$.
[h] MI: PB*i*BEM$_{1632}$.

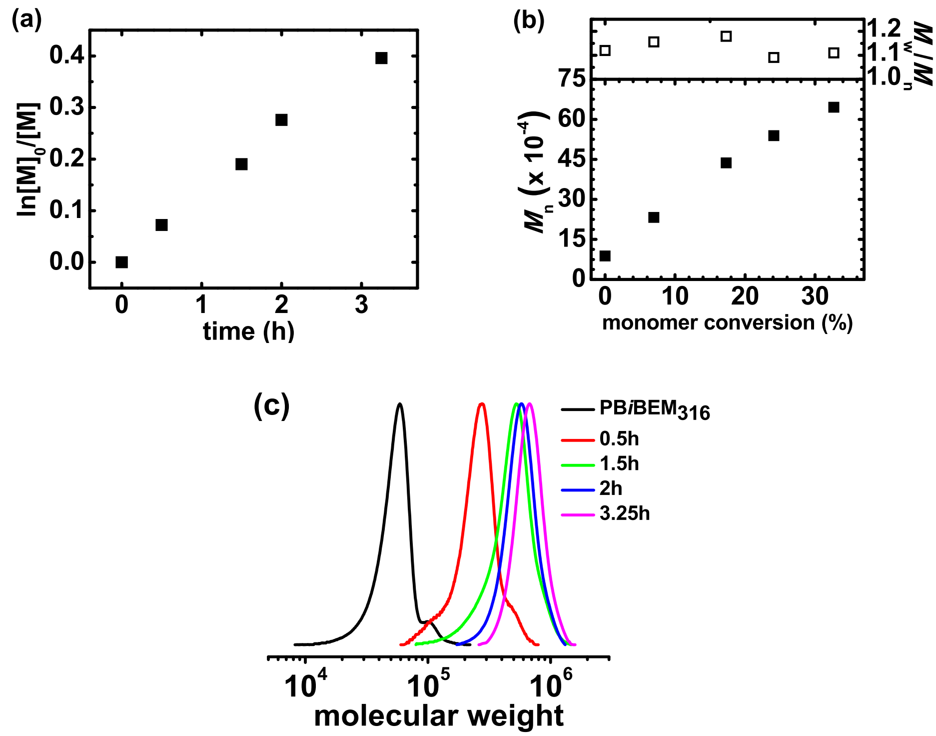

Fig. 2. Preparation of macromolecular bottlebrushes with the use of PB*i*BEM$_{316}$: (a) first-order kinetic plot of monomer conversion *vs.* time, (b) M_n and M_w/M_n *vs.* monomer conversion; (c) GPC traces of BA polymerization according to Table 2, entry 1. LMW impurities are not included for clarity, but can be found in Fig. S13d.

experiments were used to assess overall control of polymerization (Fig. S13c and S14c for **B1** and **B2**, respectively). The mixture of cleaved sidechains and LMW impurities had low dispersity, suggesting good control in both grafting-from polymerizations.

2.3. AFM characterization of the prepared molecular brushes

AFM measurements (Fig. 4) confirmed the successful formation of molecular brushes with different degree of polymerization for the main

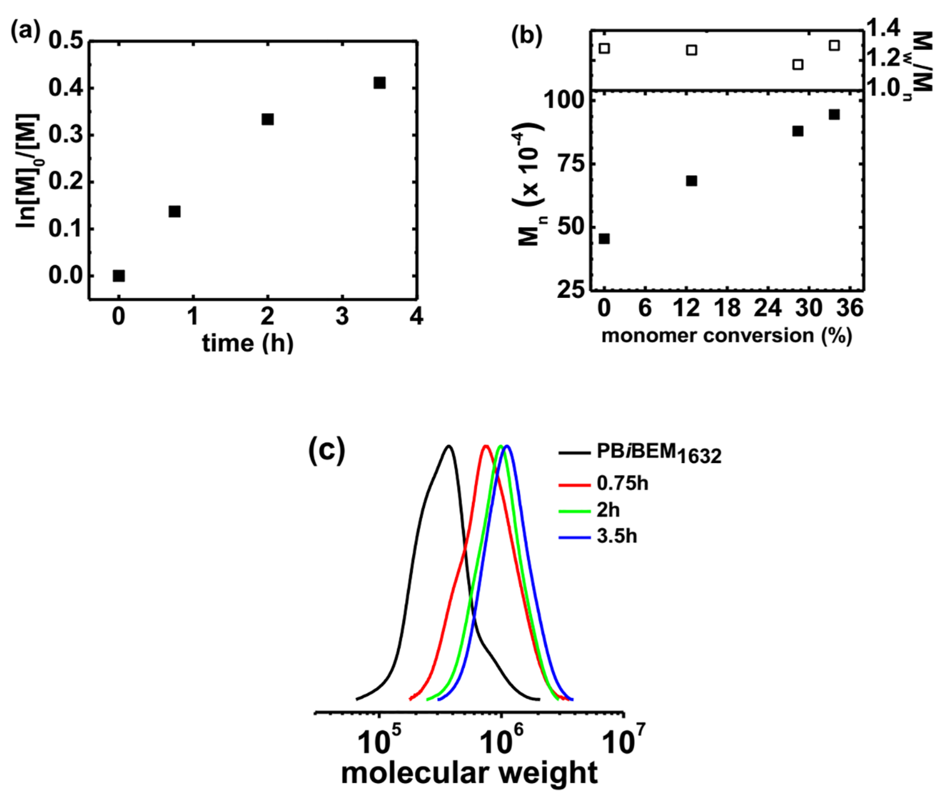

Fig. 3. Preparation of macromolecular bottlebrushes with the use of PB*i*BEM$_{1632}$: (a) first-order kinetic plot of monomer conversion *vs.* time, (b) M_n and M_w/M_n *vs.* monomer conversion; (c) GPC traces of BA polymerization according to Table 2, entry B2. LMW impurities not included for clarity, but can be found in Fig. S14d.

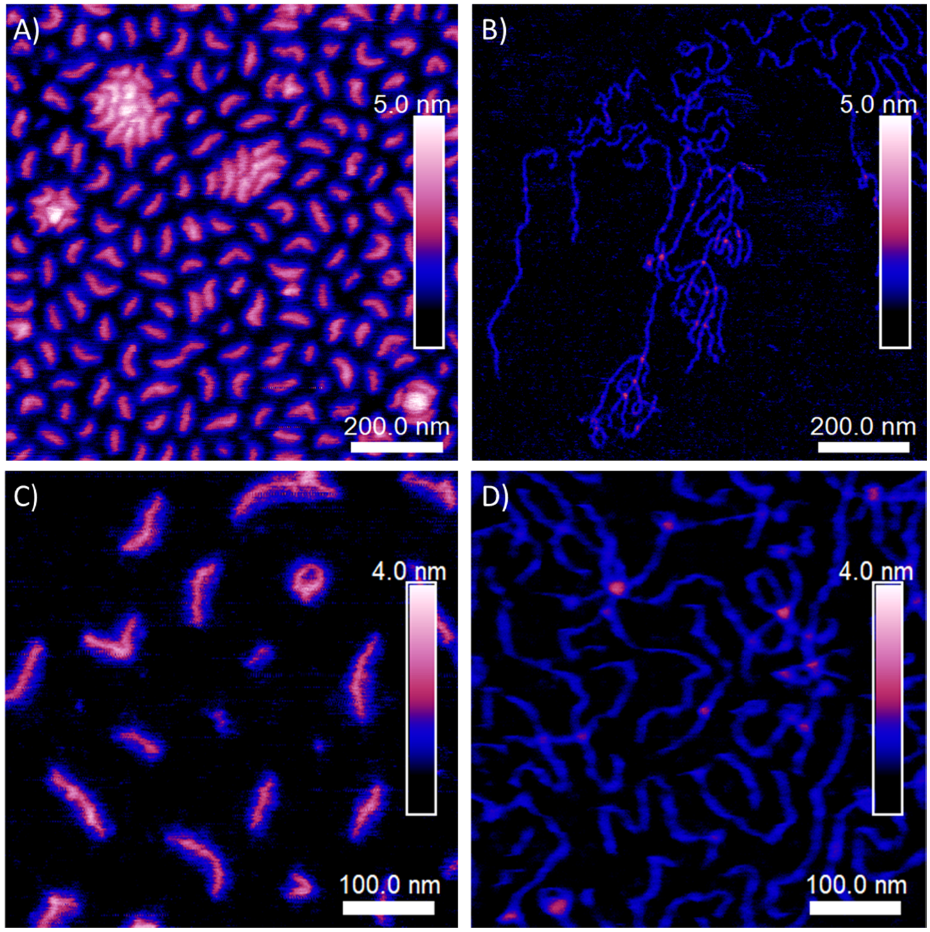

Fig. 4. AFM topography images of: (A), (C) PB*i*BEM$_{316}$-based brushes and (B), (D) PB*i*BEM$_{1632}$-based brushes spin-casted on flat silicon substrate.

backbone and grafted polymer chains. In the case of bottlebrushes prepared from PB*i*BEM$_{316}$ initiator, the number-average contour length (L_n) was 93.0 ± 8.6 nm, while the width was 48.2 ± 4.8 nm and the length distribution (L_w/L_n) of backbone was 1.01, see Figs. S17 and Table S4. If the main backbone adapted a fully extended conformation, and the length of the C—C—C monomeric unit is equal to 0.25 nm, the contour length of the bottlebrush should be around 79 nm. However, as visualized in the Fig. 4C, the main backbone is shorter than the entire molecule, and one must take into account the contribution of the side chains to the final value of the brush length.

The brushes obtained from much longer macroinitiator (PB*i*BEM$_{1632}$) had L_n value 452 ± 68 nm, Fig. 4B and D, Table S4), which correlates well with the results obtained for shorter molecules. However, the PB*i*BEM$_{1632}$-based brushes were much thinner, due to lower DP of the side chains with the average width = 17.2 ± 2 nm, Fig. S17C. The L_w/L_n was calculated to be 1.03 (Table S4).

3. Conclusion

Star and molecular bottlebrush polymers with poly(*n*-butyl acrylate) side chains were prepared by *se*ATRP using ca. 100 ppm of copper catalyst. A more negative applied potential resulted in faster controlled polymerization. Applied potentials more negative than E_{pc}-140 mV caused a decrease in polymerization rate and loss of control. An applied potential of E_{pc}-80 mV provided the fastest polymerization and small contribution of radical termination. This resulted in sucrose-based star polymers with low dispersity of both star polymers (M_w/M_n = 1.11) and cleaved arms (M_w/M_n = 1.04), as well as molecular bottlebrushes with narrow MW distributions. Low molecular weight impurities were present in all samples and likely originated from transfer reactions or arm cleavage. The electric current as an external stimulus was proved is a useful synthetic tool which can be used to prepare advanced materials with desired functions and properties.

Declaration of Competing Interest

The authors declare that they have no known competing financial interests or personal relationships that could have appeared to influence the work reported in this paper.

Acknowledgements

Financial support from NSF (DMR 1501324, CMMI 1663305) is gratefully acknowledged. P.C. acknowledges Minister of Science and Higher Education scholarship for outstanding young scientists (0001/E-363/STYP/13/2018).

Data availability

The raw/processed data required to reproduce these findings cannot be shared at this time due to technical or time limitations.

Appendix A. Supplementary material

Supplementary data to this article can be found online at https://doi.org/10.1016/j.eurpolymj.2020.109566.

References

[1] M. Abbasi, L. Faust, M. Wilhelm, Comb and bottlebrush polymers with superior

rheological and mechanical properties, Adv. Mater. 31 (2019) 1806484, https://doi.org/10.1002/adma.201806484.
[2] G. Xie, M.R. Martinez, M. Olszewski, S.S. Sheiko, K. Matyjaszewski, Molecular bottlebrushes as novel materials, Biomacromolecules 20 (2019) 27–54, https://doi.org/10.1021/acs.biomac.8b01171.
[3] J. Faivre, B.R. Shrestha, G. Xie, T. Delair, L. David, K. Matyjaszewski, X. Banquy, Unraveling the correlations between conformation, lubrication, and chemical stability of bottlebrush polymers at interfaces, Biomacromolecules 18 (2017) 4002–4010, https://doi.org/10.1021/acs.biomac.7b01063.
[4] S.-I. Yamamoto, J. Pietrasik, K. Matyjaszewski, ATRP synthesis of thermally responsive molecular brushes from oligo(ethylene oxide) methacrylates, Macromolecules 40 (2007) 9348–9353, https://doi.org/10.1021/ma701970t.
[5] A. Nese, N.V. Lebedeva, G. Sherwood, S. Averick, Y. Li, H. Gao, L. Peteanu, S.S. Sheiko, K. Matyjaszewski, pH-Responsive fluorescent molecular bottlebrushes prepared by atom transfer radical polymerization, Macromolecules 44 (2011) 5905–5910, https://doi.org/10.1021/ma201045c.
[6] D. Wu, A. Nese, J. Pietrasik, Y. Liang, H. He, M. Kruk, L. Huang, T. Kowalewski, K. Matyjaszewski, Preparation of polymeric nanoscale networks from cylindrical molecular bottlebrushes, ACS Nano 6 (2012) 6208–6214, https://doi.org/10.1021/nn302096d.
[7] M. Vatankhah-Varnosfaderani, A.N. Keith, Y. Cong, H. Liang, M. Rosenthal, M. Sztucki, C. Clair, S. Magonov, D.A. Ivanov, A.V. Dobrynin, S.S. Sheiko, Chameleon-like elastomers with molecularly encoded strain-adaptive stiffening and coloration, Science 359 (2018) 1509–1513, https://doi.org/10.1126/science.aar5308.
[8] T. Pakula, Y. Zhang, K. Matyjaszewski, H.-I. Lee, H. Boerner, S. Qin, G.C. Berry, Molecular brushes as super-soft elastomers, Polymer 47 (2006) 7198–7206, https://doi.org/10.1016/j.polymer.2006.05.064.
[9] M.J. Flanders, W.M. Gramlich, Reversible-addition fragmentation chain transfer (RAFT) mediated depolymerization of brush polymers, Polym. Chem. 9 (2018) 2328–2335, https://doi.org/10.1039/C8PY00446C.
[10] H.Y. Cho, P. Krys, K. Szcześniak, H. Schroeder, S. Park, S. Jurga, M. Buback, K. Matyjaszewski, Synthesis of poly(OEOMA) using macromonomers *via* "grafting-through" ATRP, Macromolecules 48 (2015) 6385–6395, https://doi.org/10.1021/acs.macromol.5b01592.
[11] W. Gan, Y. Shi, B. Jing, X. Cao, Y. Zhu, H. Gao, Produce molecular brushes with ultrahigh grafting density using accelerated CuAAC grafting-onto strategy, Macromolecules 50 (2017) 215–222, https://doi.org/10.1021/acs.macromol.6b02388.
[12] H. Gao, K. Matyjaszewski, Synthesis of molecular brushes by "grafting onto" method: Combination of ATRP and click reactions, J. Am. Chem. Soc. 129 (2007) 6633–6639, https://doi.org/10.1021/ja0711617.
[13] G. Xie, M.R. Martinez, W.F.M. Daniel, A.N. Keith, T.G. Ribelli, M. Fantin, S.S. Sheiko, K. Matyjaszewski, The benefits of catalyzed radical termination: high-yield synthesis of polyacrylate molecular bottlebrushes without gelation, Macromolecules 51 (2018) 6218–6225, https://doi.org/10.1021/acs.macromol.8b00849.
[14] J. Bernard, A. Favier, T.P. Davis, C. Barner-Kowollik, M.H. Stenzel, Synthesis of poly (vinyl alcohol) combs *via* MADIX/RAFT polymerization, Polymer 47 (2006) 1073–1080, https://doi.org/10.1016/j.polymer.2005.12.004.
[15] K. Huang, J. Rzayev, Well-defined organic nanotubes from multicomponent bottlebrush copolymers, J. Am. Chem. Soc. 131 (2009) 6880–6885, https://doi.org/10.1021/ja901936g.
[16] C. Cheng, K. Qi, E. Khoshdel, K.L. Wooley, Tandem synthesis of core–shell brush copolymers and their transformation to peripherally cross-linked and hollowed nanostructures, J. Am. Chem. Soc. 128 (2006) 6808–6809, https://doi.org/10.1021/ja061892r.
[17] C.J. Hawker, A.W. Bosman, E. Harth, New polymer synthesis by nitroxide mediated living radical polymerizations, Chem. Rev. 101 (2001) 3661–3688, https://doi.org/10.1021/cr990119u.
[18] J. Nicolas, Y. Guillaneuf, C. Lefay, D. Bertin, D. Gigmes, B. Charleux, Nitroxide-mediated polymerization, Prog. Polym. Sci. 38 (2013) 63–235, https://doi.org/10.1016/j.progpolymsci.2012.06.002.
[19] K. Matyjaszewski, J. Xia, Atom transfer radical polymerization, Chem. Rev. 101 (2001) 2921–2990, https://doi.org/10.1021/cr940534g.
[20] X. Banquy, J. Burdyńska, D.W. Lee, K. Matyjaszewski, J. Israelachvili, Bioinspired bottle-brush polymer exhibits low friction and amontons-like behavior, J. Am. Chem. Soc. 136 (2014) 6199–6202, https://doi.org/10.1021/ja501770y.
[21] Y. Wang, F. Lorandi, M. Fantin, P. Chmielarz, A.A. Isse, A. Gennaro, K. Matyjaszewski, Miniemulsion ARGET ATRP *via* interfacial and ion-pair catalysis: from ppm to ppb of residual copper, Macromolecules 50 (2017) 8417–8425, https://doi.org/10.1021/acs.macromol.7b01730.
[22] H.J.Y.J.H. Jeon, S.H. Ahn, J.H. Choi, K.S. Cho, Synthesis of high molecular weight 3-arm star PMMA by ARGET ATRP, Macromol. Res. 17 (2009) 240–244, https://doi.org/10.1007/BF03218686.
[23] J. Burdyńska, H.Y. Cho, L. Mueller, K. Matyjaszewski, Synthesis of star polymers using ARGET ATRP, Macromolecules 43 (2010) 9227–9229, https://doi.org/10.1021/ma101971z.
[24] A. Nese, Y. Li, S.S. Sheiko, K. Matyjaszewski, Synthesis of molecular bottlebrushes by atom transfer radical polymerization with ppm amounts of Cu catalyst, ACS Macro Lett. 1 (2012) 991–994, https://doi.org/10.1021/mz3002484.
[25] B.G.P. van Ravensteijn, R. Bou Zerdan, M.E. Helgeson, C.J. Hawker, Minimizing star-star coupling in Cu(0)-mediated controlled radical polymerizations, Macromolecules 52 (2018) 601–609, https://doi.org/10.1021/acs.macromol.8b02375.
[26] S. Park, H.Y. Cho, K.B. Wegner, J. Burdynska, A.J.D. Magenau, H.-J. Paik, S. Jurga, K. Matyjaszewski, Star synthesis using macroinitiators *via* electrochemically mediated atom transfer radical polymerization, Macromolecules 46 (2013) 5856–5860, https://doi.org/10.1021/ma401308e.
[27] P. Chmielarz, Synthesis of α-D-glucose-based star polymers through simplified electrochemically mediated ATRP, Polymer 102 (2016) 192–198, https://doi.org/10.1016/j.polymer.2016.09.007.
[28] P. Chmielarz, S. Park, A. Sobkowiak, K. Matyjaszewski, Synthesis of β-cyclodextrin-based star polymers *via* a simplified electrochemically mediated ATRP, Polymer 88 (2016) 36–42, https://doi.org/10.1016/j.polymer.2016.02.021.
[29] P. Chmielarz, Synthesis of inositol-based star polymers through low ppm ATRP methods, Polym. Adv. Technol. 28 (2017) 1804–1812, https://doi.org/10.1002/pat.4065.
[30] I. Zaborniak, P. Chmielarz, K. Wolski, G. Grześ, A.A. Isse, A. Gennaro, S. Zapotoczny, A. Sobkowiak, Tannic acid-inspired star-like macromolecules *via* temporally controlled multi-step potential electrolysis, Macromol. Chem. Phys. 220 (2019) 1900073, https://doi.org/10.1002/macp.201900073.
[31] J. Cuthbert, S.S. Yerneni, M. Sun, T. Fu, K. Matyjaszewski, Degradable polymer stars based on tannic acid cores by ATRP, Polymers 11 (2019) 752, https://doi.org/10.3390/polym11050752.
[32] D. Neugebauer, B.S. Sumerlin, K. Matyjaszewski, B. Goodhart, S.S. Sheiko, How dense are cylindrical brushes grafted from a multifunctional macroinitiator? Polymer 45 (2004) 8173–8179, https://doi.org/10.1016/j.polymer.2004.09.069.
[33] B.S. Sumerlin, D. Neugebauer, K. Matyjaszewski, Initiation efficiency in the synthesis of molecular brushes by grafting from *via* atom transfer radical polymerization, Macromolecules 38 (2005) 702–708, https://doi.org/10.1021/ma048351b.
[34] B.S. Sumerlin, D. Neugebauer, K. Matyjaszewski, Initiation efficiency in the synthesis of molecular brushes by grafting from *via* atom transfer radical polymerization, Macromolecules 38 (2005) 702–708, https://doi.org/10.1021/ma048351b.
[35] I.N. Haugan, M.J. Maher, A.B. Chang, T.-P. Lin, R.H. Grubbs, M.A. Hillmyer, F.S. Bates, Consequences of grafting density on the linear viscoelastic behavior of graft polymers, ACS Macro Lett. 7 (2018) 525–530, https://doi.org/10.1021/acsmacrolett.8b00116.
[36] T.P. Lin, A.B. Chang, S.X. Luo, H.Y. Chen, B. Lee, R.H. Grubbs, Effects of grafting density on block polymer self-assembly: From linear to bottlebrush, ACS Nano 11 (2017) 11632–11641, https://doi.org/10.1021/acsnano.7b06664.
[37] P. Chmielarz, M. Fantin, S. Park, A.A. Isse, A. Gennaro, A. Magenau, J.D.A. Sobkowiak, K. Matyjaszewski, Electrochemically mediated atom transfer radical polymerization (*e*ATRP), Prog. Polym. Sci. 69 (2017) 47–78, https://doi.org/10.1016/j.progpolymsci.2017.02.005.
[38] M. Fantin, F. Lorandi, A. Gennaro, A.A. Isse, K. Matyjaszewski, Electron transfer reactions in atom transfer radical polymerization, Synthesis 49 (2017) 3311–3322, https://doi.org/10.1055/s-0036-1588873.
[39] L. Thevenin, C. Fliedel, K. Matyjaszewski, R. Poli, Impact of catalyzed radical termination (CRT) and reductive radical termination (RRT) in metal-mediated radical polymerization processes, Eur. J. Inorg. Chem. (2019) 4489–4499, https://doi.org/10.1002/ejic.201900901.
[40] R. Whitfield, K. Parkatzidis, M. Rolland, N.P. Truong, A. Anastasaki, Tuning dispersity by photoinduced atom transfer radical polymerisation: monomodal distributions with ppm copper concentration, Angew. Chem., Int. Ed. 58 (2019) 13323–13328, https://doi.org/10.1002/anie.201906471.
[41] P. Chmielarz, T. Pacześniak, K. Rydel-Ciszek, I. Zaborniak, P. Biedka, A. Sobkowiak, Synthesis of naturally-derived macromolecules through simplified electrochemically mediated ATRP, Beilstein J. Org. Chem. 13 (2017) 2466–2472, https://doi.org/10.3762/bjoc.13.243.